Articles

Phosphorylation and Flexibility of Cyclic-AMP-Dependent Protein Kinase (PKA) Using ^{31}P NMR Spectroscopy†

Markus H. J. Seifert,‡ Christine B. Breitenlechner,‡ Dirk Bossemeyer,§ Robert Huber,‡ Tad A. Holak,‡ and Richard A. Engh*,‡,||

Abteilung Strukturforschung, Max-Planck-Institut für Biochemie, 82152 Martinsried, Germany, and Department of Pathochemistry, German Cancer Research Center, 69120 Heidelberg, Germany, and Department of Biochemistry, Roche Diagnostics GmbH, 82377 Penzberg, Germany

Received January 7, 2002; Revised Manuscript Received March 13, 2002

ABSTRACT: Cell signaling pathways rely on phosphotransfer reactions that are catalyzed by protein kinases. The protein kinases themselves are typically regulated by phosphorylation and concurrent structural rearrangements, both near the catalytic site and elsewhere. Thus, physiological function requires posttranslational modification and deformable structures. A prototypical example is provided by cyclic AMP-dependent protein kinase (PKA). It is activated by phosphorylation, is inhomogeneously phosphorylated when expressed in bacteria, and exhibits a wide range of dynamic properties. Here we use ^{31}P nuclear magnetic resonance (NMR) spectroscopy to characterize the phosphorylation states and to estimate the flexibility of the phosphorylation sites of 2-, 3-, and 4-fold phosphorylated PKA. The phosphorylation sites Ser10, Ser139, Thr197, and Ser338 are assigned to individual NMR resonances, assisted by complexation with AMP−PNP and dephosphorylation with alkaline phosphatase. Rotational diffusion correlation times estimated from resonance line widths show progressively increasing flexibilities for phosphothreonine 197, phosphoserines 139 and 338, and disorder at phosphoserine 10, consistent with crystal structures of PKA. However, because the apparent rotational diffusion correlation time fitted for phosphothreonine 197 of the activation loop is longer than the overall PKA rotational diffusion time, microsecond to millisecond time scale conformational exchange effects involving motions of phosphothreonine 197 are probable. These may represent "open"−"closed" transitions of the uncomplexed protein in solution. These data represent direct measurements of flexibilities also associated with functional properties, such as ATP binding and membrane association, and illustrate the applicability of ^{31}P NMR for functional and dynamic characterization of protein kinase phosphorylation sites.

Activity modulation via phosphorylation is the predominant mechanism of signal transduction in cellular pathways, which, for example, control proliferation, stress response, and apoptosis. Phosphorylation and dephosphorylation events are catalyzed by protein kinases and protein phosphatases, respectively; these enzymes are themselves typically regulated by phosphorylation. Signaling cascades include also a variety of other events such that signals require a proper association of many factors, and spurious signals from spontaneous events are minimized. Failure to maintain signaling fidelity causes a variety of diseases: most cancers are associated with constitutive activation of one or more protein kinases (*1*).

Phosphorylation control of protein kinase activity occurs via different mechanisms. Phosphorylation can create recognition sites for protein kinase−protein substrate or protein kinase−protein inhibitor docking, as exemplified by phosphotyrosine−SH2 domain interactions. Phosphorylation may occur at sites that block substrate binding and thereby inactivate the kinase. Perhaps the best known mechanisms involve phosphorylation sites that activate the kinase: a generally conserved feature among protein kinases is activation by phosphorylation at the "activation loop", which when unphosphorylated may inhibit primarily by blocking access to the ATP[1] binding site or by preventing catalytically competent structuring of the active site (for recent reviews, see for example refs *2* and *3*).

† This work was supported in part by the Deutsche Forschungsgemeinschaft Grant (SFB533) and in part by a grant from the Bayerische Wirtschaftsministerium.

* Corresponding author.
‡ Max-Planck-Institut für Biochemie.
§ German Cancer Research Center.
|| Roche Diagnostics GmbH.

[1] Abbreviations: PKA, cAMP-dependent protein kinase; cAMP, cyclic adenosine-monophosphate; NMR, nuclear magnetic resonance; EDTA, ethylenediaminetetraacetic acid; DTT, dithiothreitol; MES, 2-(*N*-morpholino)ethanesulfonic acid; ATP, adenosine triphosphate; AMP−PNP, β,γ-imino-adenosine-triphosphate; AlP, alkaline phosphatase.

10.1021/bi025509g CCC: $22.00
Published on Web 04/18/2002

The properties of protein kinases present several obstacles for researchers. The intrinsic flexibilities of protein kinases may explain their tendency to form inclusion bodies in high yield expression systems, to aggregate in solution, and to resist renaturation. Phosphorylation of recombinant protein kinases may occur at nonphysiological sites or not at all. Samples are often heterogeneous with respect to overall extent of phosphorylation, phosphorylation sites; flexibility creates structural heterogeneity as well. Taken together, these properties tend to limit the capacity to generate protein for research, to complicate interpretation of experimental results, and for example to impede kinase crystallization.

In contrast to crystallography, NMR techniques are well suited to study both static and dynamic properties, even if samples are heterogeneous in composition and structure, provided that individual resonances are resolved. ^{31}P NMR spectroscopy (*4*) is thus ideally suited for studies of phosphorylated or phosphate binding molecules, and allows the identification of specific phosphorylation sites, kinetics of phosphotransfer events, or analysis of dynamic phenomena involving phosphorus, on time scales ranging from picoseconds to days. Examples include studies of amino acids (*5*), peptides (*6*), alkaline phosphatase (*7*), the complex of G-actin with ATP (*8*, *9*), flavoprotein component of the *Escherichia coli* sulfite reductase (*10*), bovine cardiac troponin T and I (*11*, *12*), and other proteins (*13*−*17*). Several studies have focused on the application of ^{31}P NMR to evaluate internal flexibilities, for example of DNA (*18*) and also of proteins (*17*, *19*). ^{31}P NMR spectroscopy has several advantages over the ^{15}N, ^{13}C relaxation studies that are now routinely used to characterize picosecond to millisecond protein backbone flexibility. First, the sample requires no isotopic labeling. Second, while analysis of ^{15}N data is complicated by the variety of possible relaxation mechanisms, a single source of relaxation, the chemical shift anisotropy (CSA), dominates for ^{31}P at higher magnetic fields (*8*, *9*, *20*). This allows a direct evaluation of internal molecular motions if the appropriate chemical shift tensor is known and if conformational exchange can be neglected. The values of the ^{31}P CSA tensor have been determined for several compounds (*21*) and thus are available for ^{31}P NMR relaxation studies (*18*, *19*). When fast conformational exchange effects are present, the peak widths are determined by a combination of internal motions, overall tumbling, and conformational exchange induced resonance broadening. In this case, conformation exchange is detectable when line widths exceed those corresponding to the overall molecular rotational correlation time (*22*). Slow conformational exchange is detectable as multiple, possibly overlapping, resonance peaks representing the different conformational states.

The 40-kDa catalytic subunit of cAMP-dependent protein kinase (PKA) has been studied intensively by X-ray crystallography; Table 1 lists structures available from the Protein Data Bank (http://www.rcsb.org/pdb/). The conserved general protein kinase fold comprises two domains. The smaller N-terminal domain consists mainly of a five-stranded β-sheet and a conserved helix (C helix). This domain is connected to the larger, mostly α-helical C-terminal domain via a linker segment that forms a purine anchoring site of the ATP binding cleft, found at the interface between the two domains. The two-domain arrangement allows hinging motions that open and close the active site cleft (*23*). Segments specific to PKA include two structures, an N-terminal helix and C-terminal extended strand, that bridge the two domains (Figure 1). Two PKA residues, Thr197 and Ser338, must be phosphorylated for full activity. Thr197, located in the activation loop near the cleft interface, as in many other protein kinases, is thought to activate PKA by anchoring the activation loop away from the active site and freeing access of substrate and also by contributing to the structuring of the catalytic residues. The activating role of the phosphorylation of Ser338 is less clear, although a Ser338Ala mutant could not be isolated from *E. coli* while the phosphorylation mimic Ser338Glu could (*24*). Two other phosphorylation sites in PKA (Ser139 and Ser10) are associated with expression in *E. coli*. Phosphorylation (*25*) or mutation (*24*) of Ser139 has no apparent effect on activity or on solubility. The behavior of Ser10 is more complex: it is found in a segment that is disordered in most crystal structures; autophosphorylation occurs here as a function of deamidation (*26*, *27*), and phosphorylation of Ser10 has no apparent effect on activity (*25*), although Ser10Ala and Ser10Glu mutants were found mostly insoluble in *E. coli* and inactive in the soluble fraction (*24*), while truncation variants are soluble and active (*28*, *29*). Solubility of PKA mutants expressed in *E. coli* is additionally correlated with the phosphorylation of Thr197, which can be achieved in trans by coexpression of the wild-type enzyme (*30*).

A wide range of flexible phenomena have been identified for PKA. Crystal structures show N- and C-terminal domain motions associated with ATP binding which open and close the ATP binding site; inhibitor binding can induce ATP binding site states intermediate between "open" and "closed", and further can induce local translations of the ATP phosphorus anchoring glycine loop and side chain motions (*31*). Additionally, fluorescence anisotropy (*32*) methods have shown rotational correlation times at specific sites. Since the standard high-resolution ^{1}H/^{13}C/^{15}N NMR spectroscopy methods are generally limited to proteins smaller than approximately 30 kDa, no protein kinase structure has been determined with NMR. However, other NMR techniques including ^{31}P methods as described above are ideally suited for protein kinase research. For protein kinases, ^{31}P NMR methods have been used to characterize substrate specificities and reaction kinetics (*33*−*35*). The analysis of the protein kinase phosphorylation sites themselves has been rare and to our knowledge limited to a 1984 study of phosphorylase kinase (*13*). In this paper, we describe the use of ^{31}P NMR spectroscopy to characterize the number of phosphorylation sites in various PKA preparations, their flexibility, and that of AMP−PNP. The sensitivity of these phosphorylation sites to pH, dephosphorylation by alkaline phosphatase, and comparisons with crystallographic data identifies local flexibility and accessibility. In particular, the phosphorylation site at Ser10 is shown to be flexible and readily accessible to dephosphorylation.

MATERIALS AND METHODS

Sample Preparation. cAMP-dependent protein kinase Cα catalytic subunit was solubly expressed in *E. coli* and purified using a PKI(*5*−*24*) affinity column as previously described (*36*). The different phosphorylated forms were separated by ion exchange chromatography (Mono-S, Pharmacia) using a LiCl gradient from 0 to 300 mM LiCl in 20mM bis-tris

Table 1: Phosphorylation of Published PKA Structures[a]

PDB ID (ref)	description	nominal resolution	phosphorylation described	phosphorylation modeled (ave phosphate B-factor in Å^2)	modeled N-terminus (B-factor)	comments
1BKX (*55*)	PKA (mouse) adenosine	2.6	10 197 338	197(60) 338(90)	Q12(70)	
1BX6 (*56*)	PKA (mouse) balanol	2.1	197 338	197(30) 338(80)	Q12(60)	
1APM (*57*)	PKA (S139A, mouse), PKI (5−24)	2.0	10 197 338	10(100) 197(20) 338(50)	S10 (side chain 100, main chain 40)	individual atoms of residue 10 including phosphate set at B-factor 99.99
1CMK (*43*)	PKA (pig), PKI (5−24, iodinated)	2.9	197 338	197(−) 338(−)	G1(−)	no B-factors refined
1CTP (*58*)	PKA (pig), PKI (5−24, di-iodinated)	2.9	197	197(20)	K7(40)	
2CPK (*40*)	PKA (mouse) PKI (5−24)	2.7	139 197 338	139(70) 197(10) 338(40)	V15(60)	pSER 139 not hydrogen bonded to protein
1ATP (*59*)	PKA (mouse), PKI (5−24), Mn_2ATP	2.2	197 338	197(30) 338(60)	V15(60)	
1JLU (*60*)	PKA (mouse), phosphoryl PKS (5−24)	2.25	197 338	197(20) 338(50)	Q12(100)	
1JBP (*60*)	PKA (mouse), ADP, PKS (5−24)	2.2	10 197 338	10(90) 197(10) 338(50)	G9(70)	individual atoms of residues 9 and 10 set at B-factor 99.99
1FOT (*29*)	PKA (yeast)	2.8	197	197(60)	N-terminal alpha helix and part of alpha-beta linker truncated.	disordered C-terminal linker, sequence lacks other mammalian PKA phosphorylation sites, Ser338 equivalent position adjacent to insertion and packs against KcD differently but at similar position, activation loop phosphate more flexible
1FMO (*61*)	PKA (mouse), adenosine, PKI (5−24)	2.2	197 338	197(20) 338(60)	E13(90)	individual main chain atoms through residue 19 set at B-factor 100
1STC (*31*)	PKA (cow), staurosporine, PKI (5−24)	2.3	197 338	197(30) 338(60)	V15(50)	
1CDK (*44*)	PKA (pig), PKI (5−24), $Mn_2AMPPNP$	2.0	197	197(30,20)	K8(50,80)	two chains in asymmetric unit
1YDR 1YDS 1YDT (*36*)	PKA (cow), PKI (5−24), H-inhibitors	2.2 2.2 2.3	10 197 338	197(10,10,20) 338(50,50,50)	V15(40,30,50)	

[a] Summary of published PKA structures. Most proteins are phosphorylated at Thr197 and Ser338. If Ser10 is phosphorylated, it is disordered or nearly so. Ser139 and Ser338 are flexible, while Thr197 exhibits very low B-factors.

propane at pH 8.5. At +4 °C, PKA is stable under these conditions for several months. The protein was concentrated to 12 mg/mL using Ultrafree 10 kDa (Millipore) immediately prior to measurement. To resolve the NMR spectroscopic peaks of the quadruply phosphorylated PKA (see below), the buffer was changed to 5 mM MES−BisTris, 70 mM LiCl, 0.1 mM EDTA, 1 mM DTT pH 6.9 and concentrated again to a final concentration of 12 mg/mL.

NMR Spectroscopy. ^{31}P NMR spectra of PKA were obtained at a temperature of 300 K with a Bruker DRX600 14.1 T spectrometer equipped with a 5 mm ^{1}H−X broadband probe head. The proton Larmor frequency of 600 MHz corresponds to a phosphorus Larmor frequency of 242 MHz. NMR measurements were done using Shigemi NMR tubes (Shigemi, Inc., PA). Typical spectra were taken with a spectral width of 8 kHz, 8000 scans per FID, 16k time domain points, a relaxation delay of 5 s, and the application of proton decoupling. Before Fourier transformation, an 8 Hz exponential line-broadening was applied to reduce spectral noise. The chemical shifts are calibrated to free inorganic phosphate in solution at pH 8.5. The contributions to phosphorus NMR line width $\Delta\nu$ can be written as $\Delta\nu = (\pi T_2^*)^{-1} = \pi^{-1}(T_{2,\mathrm{CSA}}^{-1} + T_{2,\mathrm{dipole}}^{-1} + T_{2,\mathrm{inhom}}^{-1})$. At high fields, dipole−dipole contributions can be neglected (*8*, *9*, *20*). It was estimated from the ^{31}P line widths of H_3PO_4 and AMP−PNP free in solution that the contribution of magnetic field inhomogenety is at the most on the order of 1−2 Hz, and may therefore be neglected compared to the much broader protein peaks. Proton NMR spectra were recorded routinely on all samples of PKA to survey the appropriate shimming of each protein sample and to monitor the folding of the protein throughout the experiments. Proton T_2 relaxation times were measured by a spin−echo sequence with variable echo times. To avoid H_α−H_N *J*-coupling modulation the 180° pulse was selective for amide protons. The data

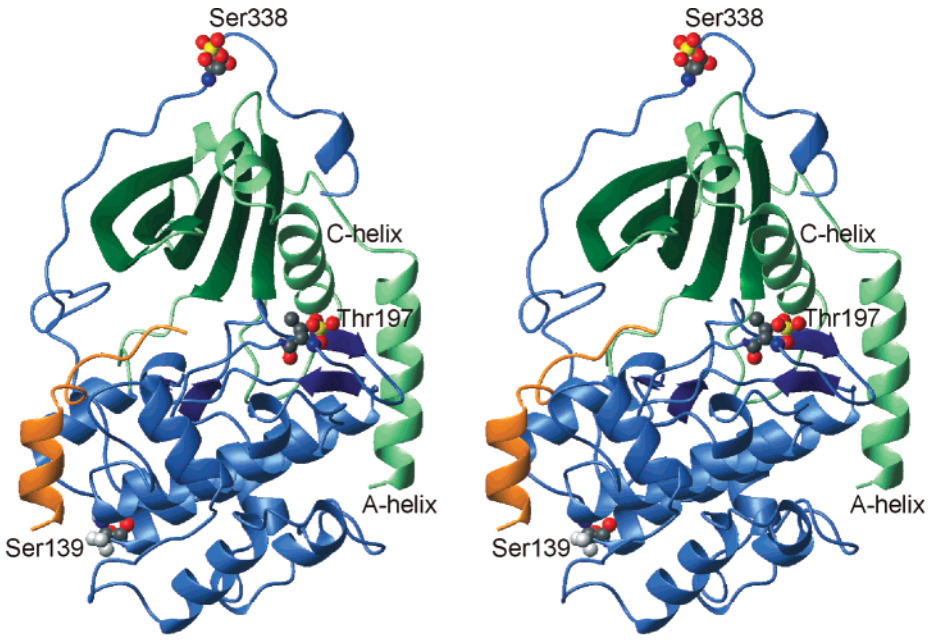

FIGURE 1: Schematic representation of PKA (taken from PDB entry 1STC), showing approximate positions of ordered phosphorylation sites. The N-terminal and C-terminal domains are shown in green and blue, respectively. Phosphorus atoms are depicted in yellow. Thr197 and Ser338, physiological phosphorylation sites, represent the ordered phosphorylation sites of most PKA structures determined to date. One structure has been published for which Ser139 is ordered and phosphorylated. Many structures report phosphorylation of Ser10, but none have been ordered so far.

were fitted with an exponential function to calculate the amide T_2.

Dephosphorylation with Alkaline Phosphatase. Prior to dephosphorylation, a ^{31}P NMR reference spectrum of 4-fold phosphorylated PKA was recorded using an experimental time of 16 h. To initiate dephosphorylation, 1 mM $MgCl_2$, 0.1 mM $ZnCl_2$ (*37*), and 0.075 U/mL calf intestinal alkaline phosphatase (AlP) (New England Biolabs) were added to the protein solution. Immediately following, a second ^{31}P NMR spectrum was recorded with identical acquisition parameters. After incomplete dephosphorylation was observed, a second identical portion of AlP was added, this time with an additional 10 mM EDTA. Four subsequent ^{31}P NMR spectra of 16 h duration each were then recorded. The effective time points of the spectra, defined by the midpoint of recording duration, are 8, 24, 40, and 56 h after adding AlP and EDTA. Proton spectra were recorded before, during, and after the experiment to monitor the folding of PKA.

Interaction with AMP−PNP. To evaluate the interaction of PKA with AMP−PNP, 0.45 mM of AMP−PNP and 0.9 mM $MgCl_2$ were added to 0.4 mM of triply phosphorylated PKA at pH 8.5. A reference spectrum of AMP−PNP alone was recorded under the same buffer conditions as the protein sample. The sweep width was 16 kHz, and 1536 scans were acquired. An exponential line broadening of 1 Hz was applied. The spectrum of PKA in combination with AMP−PNP was recorded with the same sweep width and 10 000 scans. The spectral noise of the spectrum was reduced by a exponential line broadening of 10 Hz. The line widths given in the following are corrected for the different amounts of artificial line broadening.

RESULTS

The phosphorylation sites of 2-, 3-, and 4-fold phosphorylated PKA (2P-, 3P-, and 4P-PKA, respectively) have been identified (*24*) as follows: 2P-PKA (Thr197, Ser338), 3P-PKA (Thr197, Ser338, Ser10), and 4P-PKA (Thr197, Ser338, Ser10, Ser139). As discussed in the introduction section, phosphorylation at Ser139 and at Ser10 have been identified only in *E. coli* preparations of PKA (*24*); these phosphorylations are partially suppressed in the recombinant myristoylated enzyme (A. Schlosser, A. L. Picciolo, W. Lehmann, and D. Bossemeyer, unpublished results). The ^{31}P NMR spectra of samples at pH 8.5 show three protein phosphate signals, at 1.85, 1.48, and 0.60 ppm (Figure 2). Scaling the spectra to obtain integrated intensities of unity at the 1.85 ppm peak indicates the extent of phosphorylation: the ratio of the three peak integrals becomes 1:0.5:1 in 2P-PKA, 1.0:0.9:0.9 in 3P-PKA, and 1.0:1.9:2.6 in 4P-PKA. Assuming that fractional integrated intensities arise from incomplete

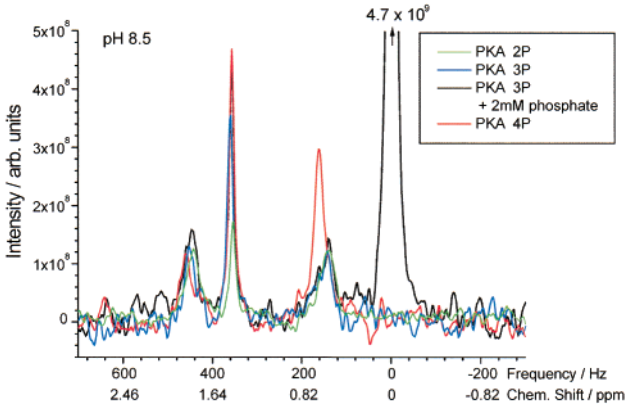

FIGURE 2: The ^{31}P NMR spectra of doubly, triply, and quadruply phosphorylated PKA at 300 K and pH 8.5 are shown. In addition, a spectrum of triply phosphorylated PKA with 2 mM phosphate added is shown. All spectra exhibit three PKA resonances: In 2P PKA, the narrow peak is significantly attenuated compared to 3P PKA. 4P PKA shows an increased intensity of the peak at 0.6 ppm. This allows the assignment of Thr197 (1.85 ppm), Ser10 (1.48 ppm), and Ser338/Ser139 (0.6 ppm).

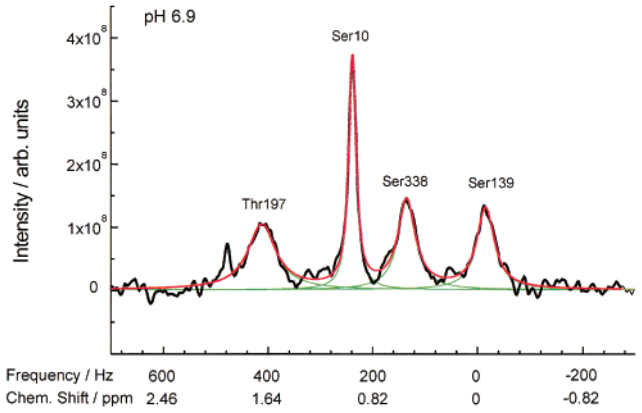

FIGURE 3: The ^{31}P NMR spectra of quadruply phosphorylated PKA at 300 K and pH 6.9 is shown. The green and red lines indicate the fitted single Lorentzian peaks and the overall fit, respectively. Thr197 shows the broadest resonance, whereas the narrowest resonance is attributed to Ser10. Ser338 and Ser139 exhibit approximately the same line width. Compared with the spectrum at pH 8.5 the resonance of Ser139 is significantly shifted.

sample separation and/or measurement errors, the peaks can be assigned to 2P-PKA (1.85, 0.60 ppm), 3P-PKA (1.85, 1.48, 0.60 ppm), and 4P-PKA (1.85, 1.48, and two at 0.60 ppm). In all spectra, the peak at 1.48 ppm is the most narrow and prominent of the protein phosphate peaks. In 2P-PKA, this is significantly reduced compared to both 3P- and 4P-PKA. 4P-PKA differs from 3P-PKA by an increase especially in the peak at 0.60 ppm. To resolve the apparent overlap of signals at 0.60 ppm, the pH was changed to 6.9; this resolved the spectra of 4P-PKA (Figure 3) by shifting one of the peaks at 0.60 to −0.03 ppm. The peak at 1.48 ppm was also shifted to 1.07 ppm, while the peak at 1.85 ppm and one of the peaks at 0.60 ppm are not shifted significantly. The peak integral ratios at pH 6.9 are 1:1:0.9:0.8.

The sample dependence, apparent flexibilities and pH sensitivities support the assignment of these peaks to the known phosphorylation sites (*24*) Thr197 (1.85 ppm), Ser10 (1.48 ppm), Ser139, and Ser338 (both 0.60 ppm). Crystal structures show that Ser10 is usually disordered (Table 1) and therefore consistent with the narrow width of the 1.48 ppm peak and also its sensitivity to pH. The appearance of the peak representing Ser10 in 2P-PKA is likely due to residual populations of 3P-PKA, while the nearly doubled intensity seen 4P-PKA (pH 8.5) may be due in part to an underestimation of the peak area of the 1.85 ppm peak. Crystal structures of mammalian PKA show the phosphate group at Thr197 to be uniformly bound to neighboring charged groups, thus less sensitive to pH shifts, rigid, and chemically distinct from phosphoserine, supporting the assignment to the 1.85 ppm peak. Ser338 and Ser139 therefore represent the 0.60 ppm peaks. One structure of PKA phosphorylated at serine 139 is available; no intramolecular hydrogen bonding to the phosphate group is apparent. Many PKA structures with phosphoserine 338 show partial shielding of the phosphate from solvent interactions by a local hydrogen bonding network involving side chains of adjoining residues (Arg336−Lys342). Thus, the relatively pH insensitive peak at 0.60 ppm (pH 8.5 and 6.9) is more likely due to Ser338, and the pH-sensitive resonance at 0.60 ppm (pH 8.5) and 0.03 ppm (pH 6.9) is likely due to Ser139; this pH sensitivity is consistent with model measurements on the isolated amino acid phosphoserine (*5*).

Alkaline phosphatase (AlP) dephosphorylation (Figure 4) experiments also support this assignment. The most rapid and obvious effect is the reduction of the narrow peak at 1.3 ppm corresponding to Ser10. After 16 h, dephosphorylation is incomplete; the 60% residual peak is slightly shifted. The peak assigned to Thr197 remains unaffected to within signal-to-noise limits, while the Ser139 and Ser338 peaks appear slightly shifted. No peak corresponding to unbound phosphate can be observed. EDTA (which dephosphorylates and reactivates phosphate bound phosphatase) and AlP was added to continue dephosphorylation (Figure 4B). After 16 h, the peaks representing disordered phosphoserine 10 and

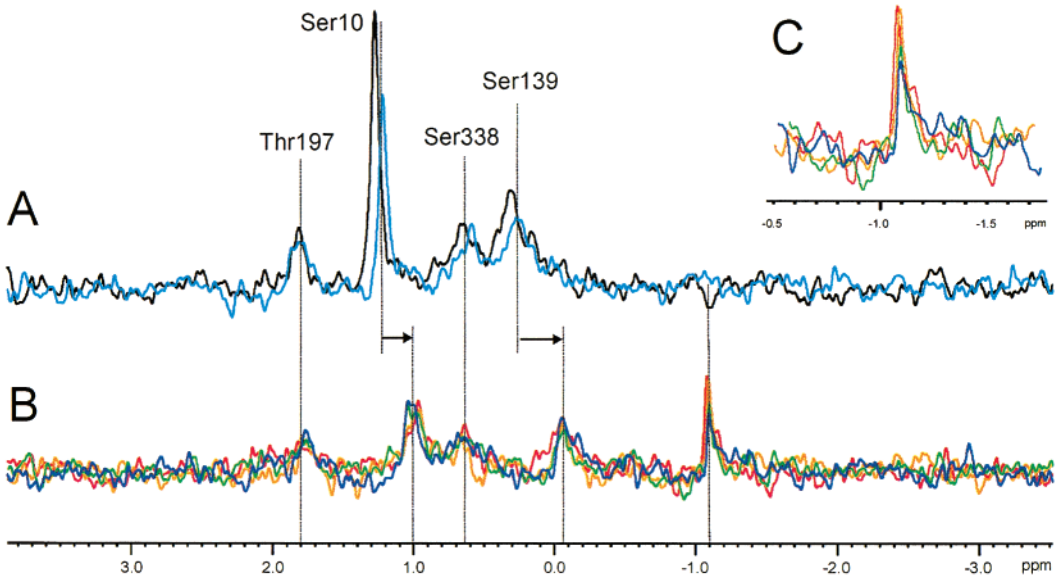

FIGURE 4: The ^{31}P NMR spectra of quadruply phosphorylated PKA in reaction with alkaline phosphatase (AlP) at 300 K are shown. The pH of the sample is approximately 6.9. The spectra before and after (midpoint: 8 h) addition of AlP are shown in black and blue, respectively. The spectra 8, 24, 40, and 56 h after addition of AlP and EDTA are shown in purple, green, orange, and red, respectively. The inset C shows the increasing peak of free phosphate. Ser10 is most susceptible to dephosphorylation, followed by Ser139 and Ser338. Thr197 is relatively resistant to dephosphorylation.

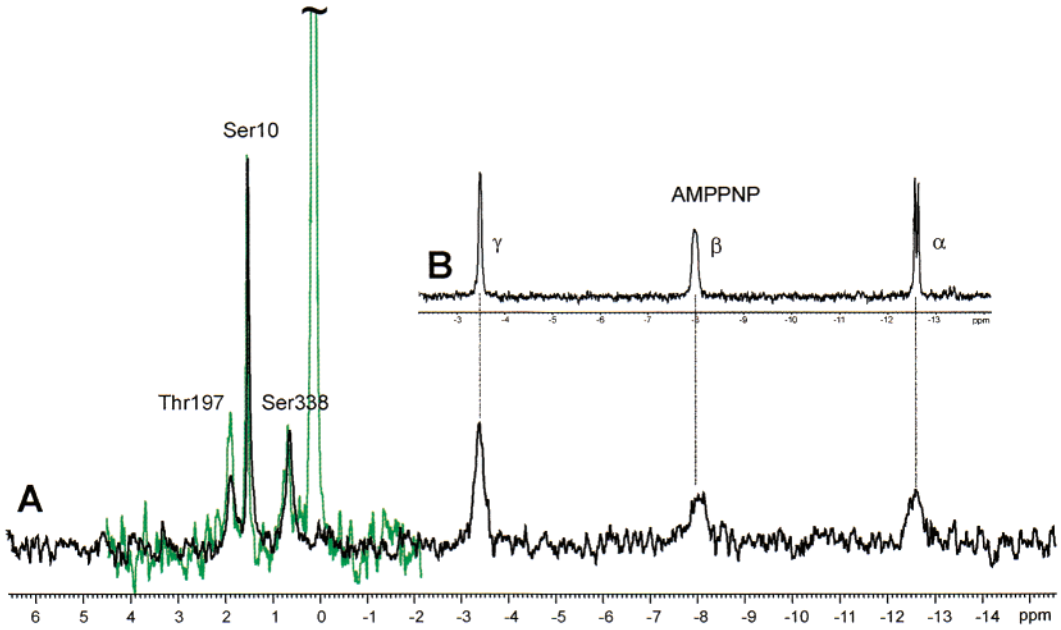

FIGURE 5: ^{31}P NMR spectrum of triply phosphorylated PKA with addition of AMP−PNP (black) and the reference spectrum of triply phosphorylated PKA with 2 mM phosphate (green) are shown. The resonance of free phosphate is shown in the inset. The spectra are scaled such that the resonances of Ser10 and Ser338 are superimposed. Interaction with PKA broadens the AMP−PNP resonances significantly. Ser10 and Ser338 of 3P PKA are not affected by AMP−PNP binding. The resonance of Thr197 is broadened upon AMP−PNP binding.

serine 139 are either reduced and shifted or supplanted by a new peak, possibly the AlP phosphorylation peak. The effect of EDTA in freeing the phosphate bound to AlP leads to the appearance of a free phosphate peak at −1.1 ppm. Thr197 and Ser338 peaks appear reduced relative to noise but unshifted. The proton NMR spectra routinely recorded before, during, and after these measurements verified the continued integrity of the PKA and eliminates denaturation as a cause of peak shifts. In summary, these results corroborate the assignment of the individual residues because Thr197 and Ser338 are the phosphorylation sites most resistant to dephosphorylation (*38*).

When AMP−PNP is added to triply phosphorylated PKA, three new peaks appear in the ^{31}P NMR spectrum, found at −3.4, −7.9, and −12.6 ppm (Figure 5). These resonances can be attributed to the γ, β, and α phosphorus atoms of AMP−PNP, respectively (*20*). These resonances exhibit the same chemical shifts as observed for pure AMP−PNP, but are significantly broadened. The doublets of the α and β resonances of pure AMP−PNP with line widths of (7.0 ± 0.2) Hz, (5.3 ± 0.3) Hz (α), and (17 ± 1) Hz, (15 ± 1) Hz (β) collapse into singlets of (69 ± 5) Hz and (99 ± 7) Hz line widths, respectively. The singlet of the γ resonance is broadened from (14.1 ± 0.3) Hz to (40 ± 2) Hz upon binding to PKA. No narrow peaks of unbound AMP−PNP are observed. The PKA resonance of Thr197 shows a line width of (43 ± 3) Hz, which is significantly broader compared to the line width of (33 ± 2) Hz in the reference spectrum. This implies that the binding of AMP−PNP to PKA has an impact on the conformation or structural flexibility around residue Thr197. This finding further corroborates the assignment of Thr197, since Ser338 is located quite distant from the ATP binding site.

The NMR relaxation parameters were extracted from the spectrum 4P-PKA at pH 6.5. The fit with Lorentzian peaks gives the line width and relaxation time T_2 values summarized in Table 2. Since the CSA is the dominating relaxation mechanism for ^{31}P at higher fields the corresponding correlation times τ_c can be calculated directly from the measured line widths $\Delta\nu$, if the contribution of magnetic field inhomogenety to line width can be neglected (*8*, *9*):

Table 2: Summary of ^{31}P Relaxation Data[a]

peak	chem shift (ppm)	line width (Hz)	T_2^* (ms)	CSA (AMP) τ_c (ns)	CSA (HPA2) τ_c (ns)
THR 197	1.77	56.7 ± 2.6	5.6 ± 0.2	45	90
SER 10	1.07	8.71 ± 0.36	37 ± 1	6.9	14
SER 338	0.66	32.0 ± 1.4	9.9 ± 0.4	25	51
SER 139	−0.03	32.2 ± 1.6	9.9 ± 0.4	25	51

[a] Summary of the measured ^{31}P chemical shifts, line widths, and relaxation times T_2^* and of the calculated correlation times for PKA at 300 K and pH 6.9. AMP and HPA2 were used as model compounds for the CSA tensor of phosphoserine/threonine. The experimental errors are given by the statistical error of line width fitting.

$$\tau_C = \left[\frac{4}{45\pi}\omega_P^2(\Delta\sigma)^2\left(1+\frac{\eta^2}{3}\right)\right]^{-1}\Delta\upsilon$$

where $\omega_P/2\pi$ is the ^{31}P Larmor frequency, η the asymmetry term of the chemical shift tensor, and $\Delta\sigma$ is the anisotropy of the chemical shift. This formula is valid for molecules with rotational diffusion in the nonextreme narrowing limit, which is applicable for proteins of the size of PKA. The calculated effective correlation times depend strongly on the asymmetry and anisotropy terms, and reflect a model of spherically symmetrical diffusive rotational motion. Line widths may be influenced by flexible phenomena that deviate significantly from this model, such as conformational exchange, and strongly constrained motions. These must be considered for correct interpretation of the effective correlation times. To bracket the range of possible effective rotational correlation times, two sets of values for the CSA

tensors were chosen for our estimates (Table 2), specifically adenosine-monophosphate (AMP) and the phospholipid HPA2 (1-hexadecyl-2-deoxyglycerophosphoric acid monohydrate, *39*). The AMP CSA tensor has an asymmetry of $\eta = 0.82$ and an anisotropy of $\Delta\sigma = 126$ ppm (*8*, *9*). The HPA2 CSA tensor is characterized by has an asymmetry of $\eta = 1.001$ and an anisotropy of $\Delta\sigma = 84.7$ ppm (*39*). Most of the published CSA tensor values for phosphocompounds cluster around $\Delta\sigma = 100$ ppm, so the true values for phosphothreonine and phosphoserine are likely to lie between the AMP and HPA2 values. When compared to the overall molecular rotational correlation time, the calculated values of $\tau_{c,eff}$ can indicate both internal flexibility (line narrowing) and conformation exchange (line broadening).

DISCUSSION

Assignment. As discussed above, the assignment of the resonances is nearly unambiguous given the differences observed between 2-, 3-, and 4-fold phosphorylated preparations of PKA and the effects of dephosphorylation and AMP−PNP binding. The assignment of Thr197 and Ser338 to peaks 1.85 and 0.60 ppm, respectively, is based on several considerations (see Figure 2). First, phosphothreonine is expected to be generally distinct from phosphoserine and an overlap is thus unlikely. Second, the sensitivity of the 1.85 ppm peak characteristics to AMP−PNP binding implies greater proximity to the binding site. Finally, the relative insensitivity of these peaks to pH induced shifts and dephosphorylation reflects the greater extent of hydrogen bonding interactions of these phosphates with the protein and experimental data (see Table 1). The assignment of Ser10 to the narrow peak at 1.48 ppm is consistent with the disorder of this residues in all crystal structures and with comparisons of integrated intensities with known phosphorylation positions of 2P-PKA, 3P-PKA, and 4P-PKA (*24*). Evidence of partial phosphorylation of this peak in the 2P-PKA sample is consistent with data showing in vitro autophosphorylation of this peak over time (*26*). The assignment of Ser139 to a pH sensitive peak at 0.60 ppm is consistent with its solvent accessibility (*40*, PDB: 2CPK) and with the distribution of peak intensities among the PKA samples.

Flexibility. As listed in Table 2, threonine 197, serines 139 and 338, and serine 10 show progressively shorter rotational correlation times. The numerical values of these times depend on the model for the CSA tensor, so two extremes for the model were chosen to bracket the true physical values. Assuming at first no conformational exchange effects (see below), Thr197 exhibits an effective rotational correlation time in the range of 45 to 90 ns, Ser338 and Ser139 equivalent at 25 to 50 ns, and Ser10 at 7 to 14 ns. This progression of apparent flexibility is roughly parallel to the progression of temperature factors refined for PKA structures (Table 1). Given the theoretical relationship between refined B-factors and average atomic displacement:

$$B = \frac{8}{3}\pi^2\langle\Delta u^2\rangle$$

the crystal structures estimate average RMS displacements from equilibrium positions for the phosphate groups to be around 0.9 Å (B = ca. 20 Å^2) for Thr197, 1.5 Å (B = ca. 60 Å^2) for Ser338, 1.6 Å (B = 70 Å^2 in 2CPK) for Ser139, and greater than 1.9 Å for Ser10 (B set at 100 Å^2 when modeled at all). Since B-factors include effects of crystalline disorder, partial occupancy, measurement errors, and underdetermination effects in addition to dynamic thermal displacement effects, estimated values typically overestimate dynamic physical displacements. However, they do show the phosphates at Thr197 to be highly ordered, at Ser338 (and Ser139) to be flexible, and at Ser10 to be highly disordered.

For a protein of 40 kDa, the overall tumbling correlation time in solution as estimated from the Stokes−Einstein equation (*41*) is expected to be around 20 ns for a rigid spherical molecule and longer if deviations from a spherical shape and rigidity are significant. Fluorescence anisotropy measurements on PKA provided rotational correlation time estimates for PKA of around 25 ns (*32*). We measure amide proton T_2 relaxation times of 5 ms to provide an estimate of the overall rotational correlation time of 40 ns using the relationship $\tau_c \approx 1/(5 \times 10^9\ T_2)$ (*42*). This estimate represents an upper limit for τ_c, considering that accuracy of the estimation method and possible aggregation effects of the relatively high concentration of protein. The overall correlation time was subsequently determined by ISN relaxation measurements on an ISN Gly−Ser labelled PKA sample to be 24 ns (data not shown). In any case, the effective rotational correlation time estimate for Thr197 is 45−90 ns longer than the overall rotational diffusion time, if not corrected for effects of conformational exchange broadening. Thus, Thr197 of uncomplexed PKA in solution appears to adopt two or more conformational states which exchange on a time scale of micro- to milliseconds.

The phosphorus atoms of Ser139 and Ser338 are relatively rigid, as they show rotational correlation times similar to the same time scale of overall tumbling. This is in apparent contrast to the relatively high degree of flexibility shown by the crystal structures (see above). However, the rapid motions that contribute to the crystallographic B-factors include translational motion components which contribute little to chemical shift anisotropy relaxation. This is particularly true for Ser338 since it is anchored by hydrogen bonds to neighboring residues. Since little crystallographic information is available regarding phosphoserine 139, we can speculate that rotamer transitions are relatively rare. Shorter correlation times relative to the overall correlation time must be attributed to fast internal motions. The residue Ser10 has been shown to the shortest correlation time of only τ_c = 7−14 ns. It has therefore a highly flexible phosphorus atom. Although this flexibility could arise from a range of internal motions, it is most likely due to a flexible protein backbone at the N-terminus, corresponding to its disorder in most of the crystal structures (see Table 1).

Flexibility and Function. (a) *Open−Closed States.* A broad range of flexibilities (dynamic and/or plastic) have been demonstrated for kinases, including ligand induced side chain motions, reorientations of the ATP binding glycine flap, refolding transitions of the activation loop as a function of phosphorylation, and open-closed transitions of N- and C-terminal domains (for reviews and references, see e.g., refs *2* and *3*). Motions of the latter type are associated with ligand, substrate, and inhibitor binding, and are though important for ATP association and ADP dissociation. For PKA, crystal structures have shown open, closed, and intermediate states, whereby closed states are typically ATP

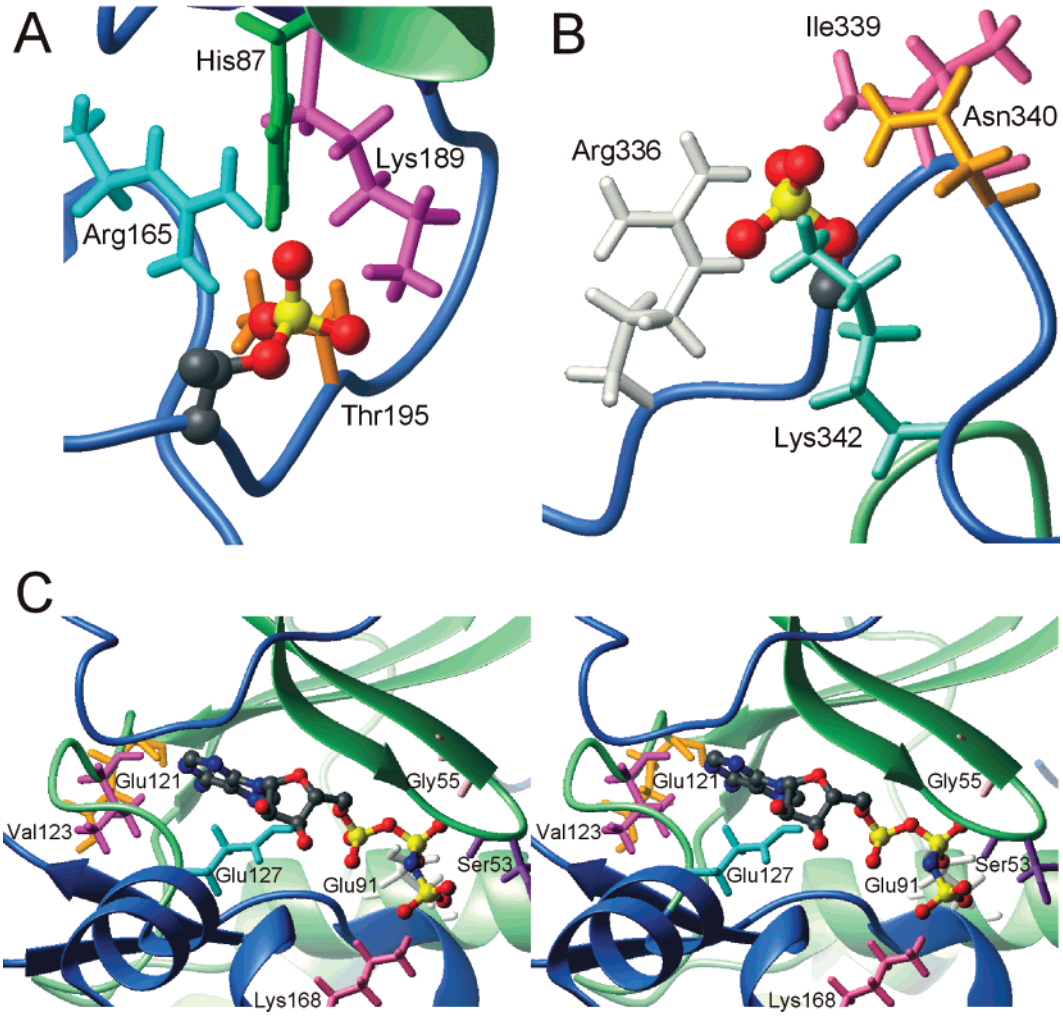

FIGURE 6: Protein environments of Thr197 (A), Ser338 (B), and of the AMP−PNP binding site (C). Panels A and B show PKA in complex with staurosporine (PDB entry 1STC). C depicts PKA in complex with PKI and AMP−PNP (PDB entry 1CDK). Thr197 mainly interacts with Arg165, His87, and Lys189. The distance between Thr197 and His87 is one measure for the open or closed conformation. The phosphate group of Ser338 is hydrogen bonded to side chains of neighboring residues Arg336, Ile339, Asn340, and Lys342. The AMP−PNP binding site is located between the two lobes of PKA. The main residues interacting with AMP−PNP are Ser53, Gly55, Glu91, Glu121, Val123, Glu127, and Lys168.

or ATP mimic bound, open are unbound, and intermediate states have been found with nonphysiological inhibitor complexes. Thus, especially the uncomplexed catalytic subunit in solution may be in equilibrium between several conformational states (*43*). No unphosphorylated PKA structures have been determined, so the precise structural role of activating phosphorylation is unknown for this enzyme. In general, the phosphorylation of activation segment residues such as Thr197 may have a role in the correct orientation of catalytic residues (*44*) and, perhaps more importantly, may help in the formation of a P+1 substrate binding site at the C-terminal end of the activation segment (*45*, *46*). The transition between open and closed states (*23*) involves alteration of the hydrogen bonding pattern of phosphothreonine 197. In the closed state, a hydrogen bond between the Thr197 phosphate group and the side chain of His87 exists, possibly helping to orient helix C (residues 84−97) into a catalytic conformation. A transition to an open state involves a loss of this hydrogen bond while the N- and C-terminal domains rotate apart. The direct involvement of the phosphate group of Thr197 in this transition makes the open−closed transition a likely cause of the conformational exchange observed for the Thr197 residue. Since no crystal structure of the monomeric or unphosphorylated PKA has been determined, precise structures for these states remain speculative. If they are intrinsically dynamic, crystallization may be hindered and crystal structures might represent only frozen conformations. Further studies on PKA in solution are required to clarify these issues.

(b) N-Terminus. The N-terminus of PKA is subject to a variety of co- and posttranslational modifications, such as the myristylation of the N-terminal glycine residue, and the deamidation of Asn2 to Asp2 and Iso-Asp2 in one-third of the mammalian Cα and Cβ enzyme populations (*27*, *47*). Phosphorylation of Ser10 has not been observed so far in enzyme isolated form mammalian sources. Deamidation of Asn2, however, results in Ser10 phosphorylation upon addition of MgATP in vitro (*26*). and thus the structure of the second N-terminal residue determines the substrate character of Ser10. Other circumstantial evidence might suggest a physiological role for phosphorylation at serine 10. The protein kinase SRC possesses a similar myristylation motif at its N-terminus containing a phosphorylation site which controls release from membranes (*48*). Both deamidation (*49*) or (de)phosphorylation are reminiscent of a "myristoyl-electrostatic switch" (*50*). Myristylated PKA in

the regulatory PKA-RII complex binds micelles in vitro, possibly via RII induced structural changes in the catalytic domain (*51*). The phosphorylation site and residues compatible with the RRxS consensus sequence for PKA phosphorylation are highly conserved across species and isoforms (*52*). No PKA structure has been fully ordered at the N-terminus. The beginning of the N-terminal helix has been shown to depend on myristylation or on the presence of detergent, either of which is associated with an alpha helix beginning at residue 10. In the absence of myristylation or detergent, the alpha helix begins one turn later. It has been shown further that phosphorylation of Ser10 in peptides results in a destabilization of turn structure (under polar conditions) and helix (under apolar conditions) (*53*). The fragmentary nature of these observations do not identify physiological roles for myristylation, Ser10 phosphorylation, or flexibility at the N-terminus. They do however demonstrate the usefulness of ^{31}P NMR to probe flexibility in this region to clarify these phenomena.

The function and activating mechanism of Ser338 is unknown at present. It has been proposed to anchor the C-terminus of PKA onto the surface of the small lobe (*23*), although the crystal structures do not indicate direct interactions of the Ser338 phosphoryl group with N-lobe residues. However, the hydrogen bonding network with neighboring residues in the C-terminal strand may have an effect in structuring the segment and modulating the binding affinities to the N-lobe. The low flexibility indicated by this work, along with the generally conserved structures in the crystal structures, supports this interpretation. Other effects could include a role in substrate protein recognition, but there is at present no experimental evidence for this.

(c) Dephosphorylation. Ser10 and Ser139 are shown to be most susceptible for dephosphorylation by alkaline phosphatase. This corresponds also to the relative sensitivities of their chemical shifts to pH change, and completes a coherent picture of greater flexibility and accessibility of these phosphates with no known physiological function, in contrast to Thr197 and Ser338 phosphates with their clear physiological roles. That Ser338 has limited susceptibility to dephosphorylation has long been known (*38*, *54*). No physiological role for phosphorylation at Ser10 or at Ser139 has been identified, as discussed above. However, higher susceptibility to phosphatase action may hinder discovery of any physiological relevance, especially if rapid phosphatase action is required physiologically to suppress any necessarily short-lived signals. The ability of ^{31}P NMR to monitor phosphorylation- dephosphorylation reactions may prove valuable in studying any new kinase/substrate interactions suggested by other lines of evidence.

(d) Binding of AMP−PNP. Although Thr197 is not directly involved in AMP−PNP binding, the Thr197 ^{31}P resonance is broadened upon AMP−PNP binding, verifying the impact of AMP−PNP binding on nearby conformational properties. In the absence of conformational exchange, line broadening would indicate rigidification of the phosphate. Crystal structures of PKA show the open and closed domain orientation states to be related to ATP site ligands unbound and bound states, respectively. The transition from the open to the closed state is also accompanied by an addition of an interaction with His87 to the Thr197 phosphate−Arg165−Lys189 network (Figure 6). Thus, rigidification of the phosphate and indeed the relative domain position upon AMP−PNP binding would be plausible. However, as discussed above, the apparent rotational diffusion time is significantly longer than the estimated overall tumbling time, strongly suggesting the presence of conformational exchange effects. Peak broadening may thus result from alteration of the time scale conformational fluctuations, alterations of the shifts of the individual conformational states, or rigidification and thus peak broadening of the individual states. Possibly the simplest of these explanations is that the binding of AMP−PNP retards the exchange between the open and the closed forms, and thereby shifts the exchange broadening regime from the fast exchange limit toward the coalescence point, which is the point of maximum broadening (*22*).

(e) Outlook. For complete quantitative characterization of internal motions in proteins, including the full range of picosecond to second time scale phenomena, a full set of relaxation data including ^{31}P T_1, T_2, and heteronuclear Overhauser effect measurements is required. This is not generally possible for many proteins, often due to limitations in protein stability or protein production. However, the relatively simple ^{31}P NMR methods and the line-shape analysis done in this study provides a readily accessible and highly informative alternative to assess structural and dynamic properties of phosphorylated proteins. For many protein kinases, these methods can be used to quickly determine the extent and homogeneity of phosphorylation, the apparent solvent accessibility of the phosphate groups, and their apparent flexibilities. Further, ^{31}P NMR can probe effects of cofactor complexation or other modifications. For PKA, these methods will prove useful for further studies of events controlling flexibilities in particular at the N-terminus and those associated with ligand binding.

ACKNOWLEDGMENT

We thank Dr. D. Ambrosius for unwavering support, and Prof. A. Berghuis for insightful suggestions.

REFERENCES

1. Blume-Jensen, P., and Hunter, T. (2001) *Nature 411*, 355.
2. Johnson, D. A., Akamine, P., Radzio-Andzelm, E., Madhusudan, E. A., and Taylor, S. S. (2001) *Chem. Rev. 101*, 2243−2270.
3. Engh, R. A. and Bossemeyer, D. (2002) *Pharmacol. Ther.*, in press.
4. Vogel, H. J. (1989) *Methods Enzymol. 177*, Part B, 263−282.
5. Takahashi, K., Shimidzu, M., Shindo, H., Kawamoto, T., Nishi, M., Matsumoto, U., and Taniguchi, S. (1987) *J. Biochem. 101*, 1107−1114.
6. Hirai, H., Yoshioka, K., and Yamada, K. (2000) *Brain Res. Protocols 5*, 182−189.
7. Hull, W. E., Halford, S. E., Gutfreund, H., and Sykes, B. D. (1976) *Biochemistry 15*, 1547−1561.
8. Brauer, M., and Sykes, B. D. (1981) *Biochemistry 20*, 2060−2064.
9. Brauer, M., and Sykes, B. D. (1981) *Biochemistry 20*, 6767−6775.
10. Evrard, A., Zeghouf, M., Fontecave, M., Roby, C., and Coves, J. (1999) *Eur. J. Biochem. 261*, 430−437.
11. Swiderek, K., Jaquet, K., Meyer, H. E., Schächtele, C., Hofmann, F., and Heilmeyer Jr, M. G. (1990) *Eur. J. Biochem. 190*, 575−82.
12. Keane, N. E., Quirk, P. G., Gao, Y., Patchell, V. B., Perry S. V., and Levine, B. A. (1997) *Eur. J. Biochem. 248*, 329−337.

13. Kilimann, M. W., Schnackerz, K. D., and Heilmeyer Jr., L. M. (1984) *Biochemistry 23*, 112−117.
14. Hahmann, M., Maurer, T., Lorenz, M., Hengstenberg, W., Glaser, S., and Kalbitzer, H. R. (1998) *Eur. J. Biochem. 252*, 51−58.
15. Macheroux, P., Sanner, C., Buttner, H., Kieweg, V., Ruterjans, H., and Ghisla, S., (1997) *Biol. Chem. 378*, 1381−1385.
16. Eckert, B. S., and Yeagle, P. L. (1996) *Cell Motil. Cytoskeleton 33*, 30−37.
17. Williams, S. P., Sykes, B. D., and Bridger, W. A. (1985) *Biochemistry 24*, 5527−5531.
18. Shindo, H. (1980) *Biopolymers 19*, 509−522.
19. Withers, S. G., Madsen, N. B., and Sykes, B. D. (1985) *Biophys. J. 48*, 1019−1026.
20. Gorenstein, D. G., Ed. *Phosphorus-31 NMR − Principles and Applications* (1984) Academic Press, Orlando.
21. Un, S., and Klein, M. P. (1989) *J. Am. Chem. Soc. 111*, 5119−5124.
22. Sandström, J. *Dynamic NMR Spectroscopy* (1982) Academic Press, London.
23. Taylor, S. S., Radzio-Andzelm, E., Madhusudan, Cheng, X., Ten Eyck, L., and Narayana, N. (1999) *Pharmacol. Ther. 82*, 133−141.
24. Yonemoto, W., McGlone, M. L., Grant, B., and Taylor, S. S. (1997) *Protein Eng. 10*, 915−925.
25. Yonemoto, W., McGlone, M. L., Grant, B., and Taylor, S. S. (1993) *J. Biol. Chem. 268*, 18626−18632.
26. Toner-Webb, J., van Patten, S. M., Walsh, D. A., and Taylor, S. S. (1992) *J. Biol. Chem. 267*, 25174−25180.
27. Jedrzejewski, P. T., Girod, A., Tholey, A., Konig, N., Thullner, S., Kinzel, V., and Bossemeyer, D. (1998) *Protein Sci. 7*, 457−469.
28. Herberg, F. W., Zimmermann, B., McGlone, M., and Susan, S. S. (1997) *Protein Sci. 6*, 569−579.
29. Mashhoon, N., Carmel, G., Pflugrath, J. W., and Kuret, J. (2001) *Arch. Biochem. Biophys. 387*, 11.
30. Girod, A., Kinzel, V., and Bossemeyer, D. (1996) *FEBS Lett. 391* (1−2), 121−125.
31. Prade, L., Engh, R. A., Girod, A., Kinzel, V., Huber, R., and Bossemeyer, D. (1997) *Structure 5*, 1627−1637.
32. Gangal, M., Cox, S., Lew, J., Clifford, T., Garrod, S. M., Aschbaher, M., Taylor, S. S., and Johnson, D. (1998) *Biochemistry 37*, 13728−13735.
33. Kwon, Y. G., Srinivasan, J., Menelow, M., Pluskey, S. and Lawrence, D. S. (1993) *J. Biol. Chem. 268*, 16725−16729.
34. Qamar, R., Yoon, M. Y., and Cook, P. F. (1992) *Biochemistry 31*, 9986−9992.
35. Prorok, M., Sukumaran, D. K., and Lawrence, D. S. (1989) *J. Biol. Chem. 264*, 17727−17733.
36. Engh, R. A., Girod, A., Kinzel, V., Huber, R., and Bossemeyer, D. (1996) *J. Biol. Chem. 271*, 26157−26164 (1996).
37. Yeung, A. C., Glahn, P. R., and Miller, D. D. (2001) *J. Nutr. Biochem. 12*, 292−299.
38. Shoji, S., Titani, K., Demaille, J. G., and Fischer, E. H. (1979) *J. Biol. Chem. 254*, 6211−6214.
39. Hauser, H., Radloff, C., Ernst, R. R., Sundell, S., and Pascher, I. (1988) *J. Am. Chem. Soc. 110*, 1054−1058.
40. Knighton, D. R., Zheng, J., Ten Eyck, L. F., Ashford, A., Xuong, N.-H., Taylor, S. S., and Sowadski, J. M. (1991) *Science 253*, 407−414.
41. Cantor, C., and Schimmel, P. R. (1980) *Biophysical Chemistry Part II: Techniques for the Study of Biological Structure and Function*, pp 549−589, W. H. Freeman and Company, San Francisco.
42. Anglister, J., Grzesiek. S., Ren, H., Klee, C. B., and Bax, A. (1993) *J. Biomol. NMR 3*, 121−126.
43. Zheng, J., Knighton, D. R., Xuong, N.-H., Taylor, S. S., Sowadski, J. M., and Ten Eyck, L. F. (1993) *Protein Sci. 2*, 1559−1573.
44. Bossemeyer, D., Engh, R. A., Kinzel, V., Ponstingl, H., and Huber, R. (1993) *EMBO J. 12*, 849−859.
45. Engh, R. A., and Bossemeyer, D. (2001) *Adv. Enz. Reg. 41*, 121−149.
46. Hubbard, S. R. (1997) *EMBO J. 16*, 5572−5581.
47. Kinzel, V., König, N., Pipkorn, R., Bossemeyer, D., and Lehmann, W. D. (2000) *Protein Sci. 9*, 2269−2277.
48. Walker, F., deBlaquiere, J., and Burgess, A. W. (1993) *J. Biol. Chem. 268*, 19552−19558.
49. Pepperkok, R., Hotz-Wagenblatt, A., Konig, N., Girod, A., Bossemeyer, D., and Kinzel, V. (2000) *J. Cell. Biol. 148*, 715−726.
50. McLaughlin, S., and Aderem, A. (1995) *Trends Biochem. Sci. 20*, 272−276.
51. Gangal, M., Clifford, T., Deich, J., Cheng, X., Taylor, S. S., and Johnson, D. A. (1999) *Proc. Natl. Acad. Sci. U.S.A. 96*, 12394−12399.
52. Skålhegg, B. S., Witczak, O., Reinton, N., Eide, T., Eikvar, S., Collas, P., Taskén, K., Jahnsen, T., and Ørstavik, S. (1999) *J. Mol. Biol. Biotech. 1*, 49−63.
53. Tholey, A., Pipkorn, R., Bossemeyer, D., Kinzel, V., and Reed, J. (2001) *Biochemistry 40*, 225−231.
54. Chiu, Y. S., and Tao, M. (1978) *J. Biol. Chem. 253*, 7145−7148.
55. Narayana, N., Cox, S., Xuong, N.-H., Ten Eyck, L. F., and Taylor, S. S. (1997) *Structure 5*, 921−935.
56. Narayana, N., Diller, T. C., Koide, K., Bunnage, M. E., Nicolaou, K. C., Brunton, L. L., Xuong, N.-H., Ten Eyck, L. F., and Taylor, S. S. (1999) *Biochemistry 38*, 2367−2376.
57. Knighton, D. R., Bell, S. M., Zheng, J., Ten Eyck, L. F., Xuong, N.-H., Taylor, S. S., and Sowadski, J. M. (1993) *Acta Crystallogr. D49*, 357−361.
58. Karlsson, R., Zheng, J., Xuong, N.-H., Taylor, S. S., and Sowadski, J. M. (1993) *Acta Crystallogr. D49*, 381−388.
59. Zheng, J., Knighton, D. R., Ten Eyck, L. F., Karlsson, R., Xuong, N.-H., Taylor, S. S., and Sowadski, J. M. (1993) *Biochemistry 32*, 2154−2161.
60. Madhusudan Trafny, E. A., Xuong, N.-H., Adams, J. A., Ten Eyck, L. F., Taylor, S. S., and Sowadski, J. M. (1994) *Protein Sci. 3*, 176−187.
61. Narayana, N., Cox, S., Shaltiel, S., Taylor, S. S., and Xuong, N.-H. (1997) *Biochemistry 36*, 4438−4448.

BI025509G